Structure, Volume *20*

Supplemental Information

A Protein Export Pathway Involving *Escherichia coli* Porins

Gerd Prehna, Guijin Zhang, Xiandi Gong, Marek Duszyk, Mark Okon, Lawrence P. McIntosh, Joel H. Weiner, and Natalie C.J. Strynadka

Inventory of Supplemental Information

Figure S1 is related to Figure 1. This figure shows the gene complementation experiment supporting the gene deletion experiment.

Figure S2 is related to Figure 1 and Figure 2. This figure shows the *E. coli* outer membrane extraction and planar lipid bilayer control with his-tagged protein.

Figure S3 is related to Figure 3 and Figure 4. This figure shows YebF biochemical behavior during purification.

Figure S4 is related to Figure 4. This figure shows additional dynamic properties observed for YebF.

Figure S5 is related to Figure 7. This figure shows the ^{15}N HSQC of the secretion mutant K64+V66+T92 and MALDI-TOF to confirm processing by the sec-system.

Figure S6 is related to Figure 5. This figure shows the electrostatic profiles of the YebF binding partners.

Supplemental Experimental Procedures

Supplemental Figures

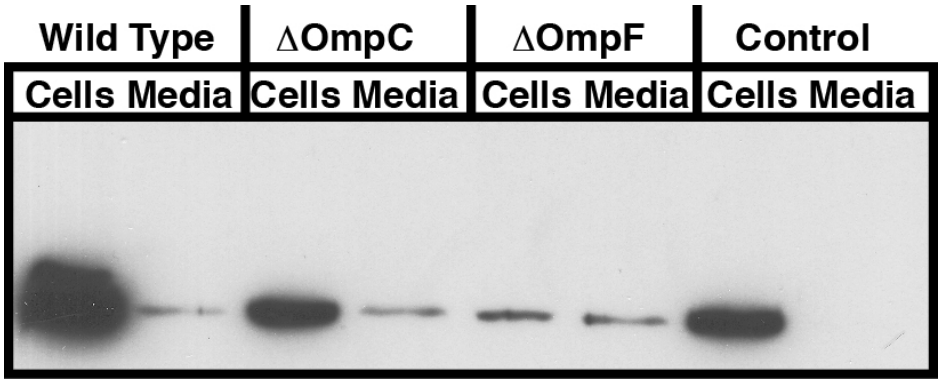

Figure S1, related to Figure 1. Complementation of Deletion Strains. A plasmid bearing the *ompF* or *ompC* gene was introduced to the corresponding deletion strain made from a BW25113 parent and YebF secretion monitored by western blot. The Wild-type experiment was perfomed with BW225113 cells. Each strain also contains the pYebFH_6MS plasmid with origin pUC. The OmpF or OmpC plasmid uses the p15A origin. The wild type lane included only the pYebFH6MS plasmid. The negative control was the non-secreting Δ*ompX* strain complemented with OmpX (HB101) p15A plasmid. Recombinant expression of OmpX disrupts the OM and reduces OmpF expression to undetectable levels (Stoorvogel et al., 1991). Cells were growth for 4 hrs. Expression variation is due to the use of kanamyacin and is dependent upon *E. coli* strain as discussed previously (Zhang et al., 2006).

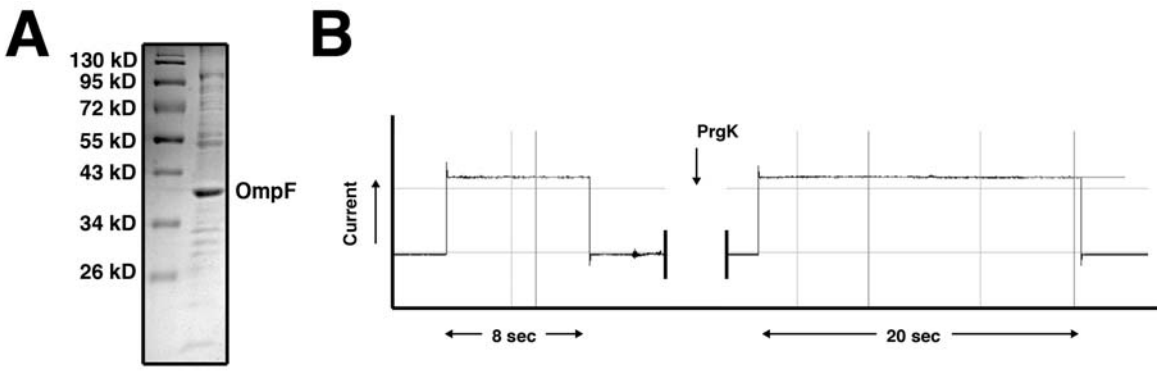

Figure S2, related to Figures 1 and 2. Planar Lipid Bilayer Control with His-tagged Protein. (A) Gel showing an outer membrane extract of *E. coli* with OmpF as one of the most abundant proteins, in line with previous literature. OmpF runs as monomer (~36 kD) when boiled. **(B)** Planar Lipid Bilayer experiment showing that his-tagged proteins do not non-specifically block the ion-conductance observed from OmpF. Channel recording was performed according to Experimental Procedures with the addition of the his-tagged protein PrgK (25 kD, soluble domain of *Salmonella spp.* type III basal body component) at the point indicated in the figure. PrgK was added in increasing concentrations up to 20-fold more than what was used in YebF experiments (400 ng/mL) with no effect on conductance.

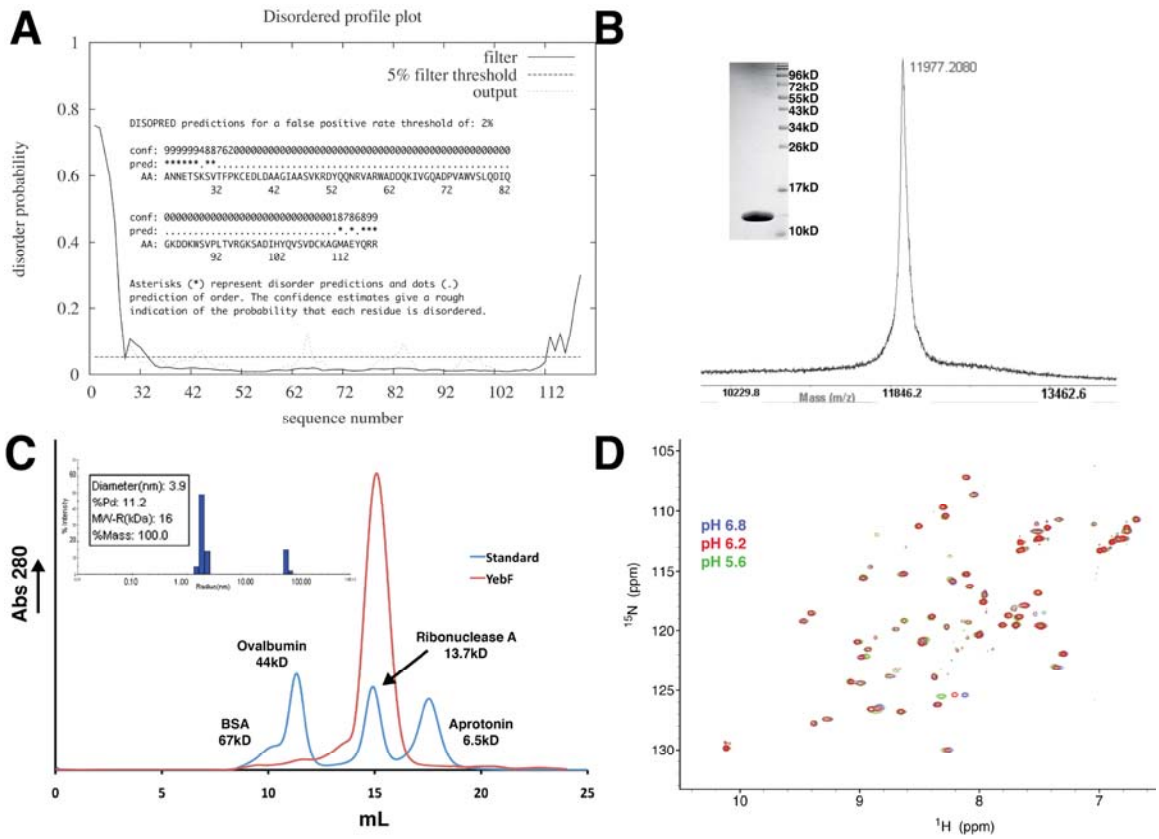

Figure S3, related to Figure 3 and Figure 4. Biophysical Characterization of YebF. **(A)** Results of disorder analysis by the server DISOPRED2. The analysis predicts that the only N-terminal residues 22-32 and the C-terminal residues 114-118 are disordered. **(B)** MALDI-ToF Mass spectrometry data of purified ^{15}N-labeled YebF showing an observed mass of 11.97kD which aggress with the theoretical mass of 11.9kD. **(C)** Calibrated gel filtration and dynamic light scattering data with purified ^{15}N-labeled YebF. %Pd indicates the percent polydispersity and MW-R(kD) the approximate molecular weight of 16kD estimated from the observed particle radius. **(D)** ^{15}N-HSQC spectra of YebF at at pH 6.8 (blue), pH 6.2 (red), and pH 5.6 (green). These spectra indicate that the missing signals are not due to rapid hydrogen exchange. That is, amide hydrogen exchange slows with decreasing pH and thus any signals missing at pH 6.8 due to this phenomenon should be observable at pH 5.6.

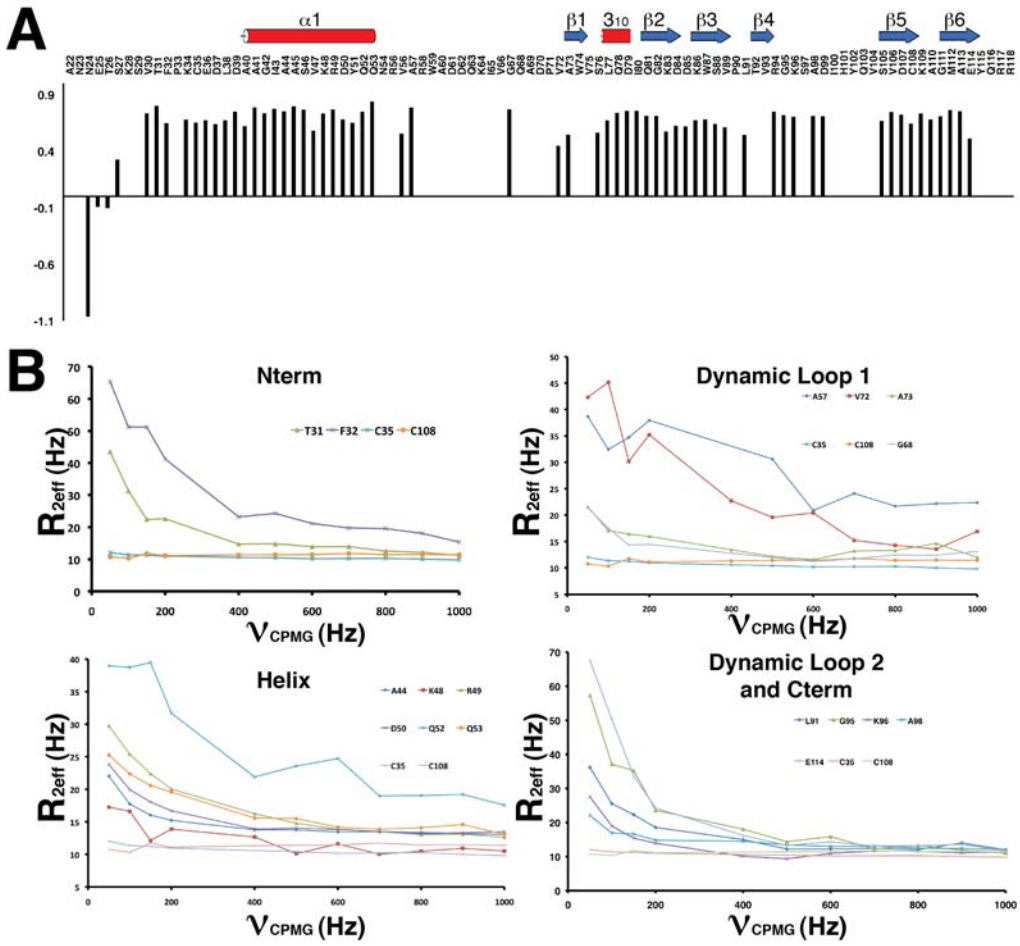

Figure S4, related to Figure 4. YebF Dynamic Residues. (A) ^{15}N NOE relaxation data for YebF recorded with a 600 MHz spectrometer at 35^{o}C (Farrow et al., 1994). Decreasing NOE values result from increasing mobility of the ^{15}N-^{1}H^{N} bond vector on the sub-nsec timescale. These data demonstrate that the N-terminus of YebF is disordered and undergoes fast conformational motions. **(B)** ^{15}N CPMG relaxation data recorded with a 600 MHz spectrometer at 35°C (Mulder et al., 2000) displaying all residues that exhibit conformational exchange broadening. The data are colored by residue, as indicated in the legend. For comparison, dispersion values recorded for residues not undergoing chemical exchange (i.e. R_{2eff} independent of $\nu_{(CPMG)}$) are included in each panel. The data are grouped together by YebF structural feature. $R_{2eff}(Hz)=-(1/T)*\ln(I\nu_{(CPMG)}/I_0)$ where T is the constant time delay (40msec), $I\nu_{(CPMG)}$ is the intensity at a given $\nu_{(CPMG)}$ value, and I_0 is the intensity of the reference spectrum.

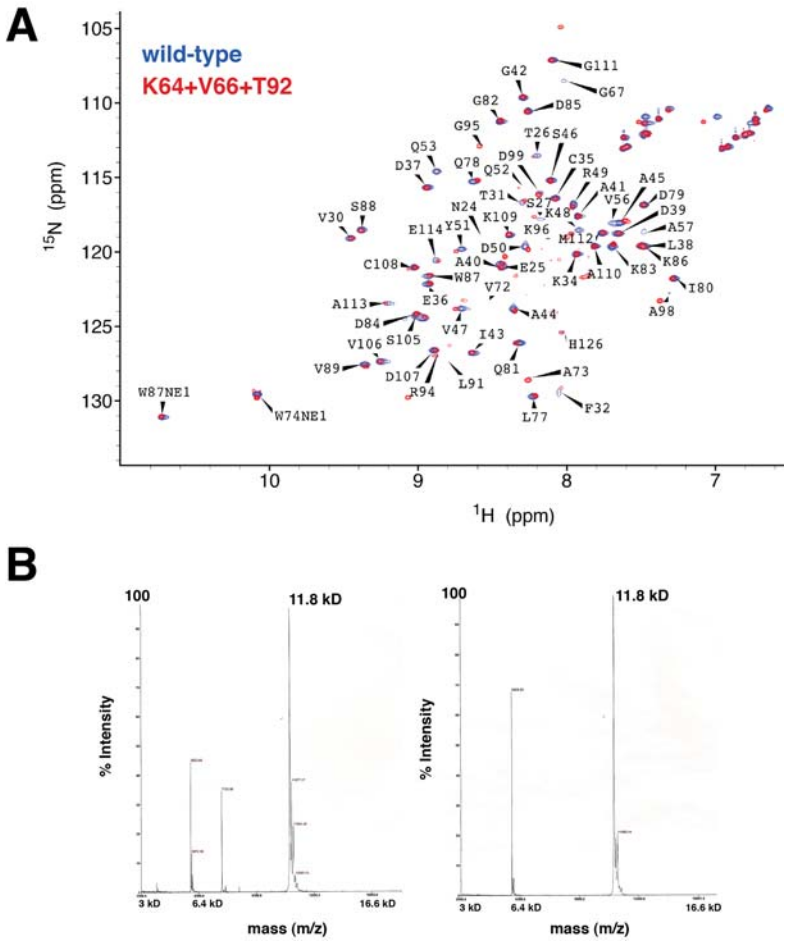

Figure S5, related to Figure 7. Stability and Processing Controls of the Secretion Variant K64+V66+T92. (A). Overlay of ^{15}N-HSQC spectra of the secretion variant with the wild-type YebF taken at 35°C. The spectra are equivalent aside from peaks near the mutated regions (eg. G67). No significant aggregation peaks appeared at 35°C, showing equivalent structure in the core and similar stability. Additionally, the disulfide was still properly formed (C35+C105 are unshifted). **(B).** Mass-spectrometry of the YebF secretion variant purified from the cell pellet (left) and media (right). Both show the same mass of 11.8 kD, as predicted for his-tagged YebF with the expected cleavage of the sec-signal.

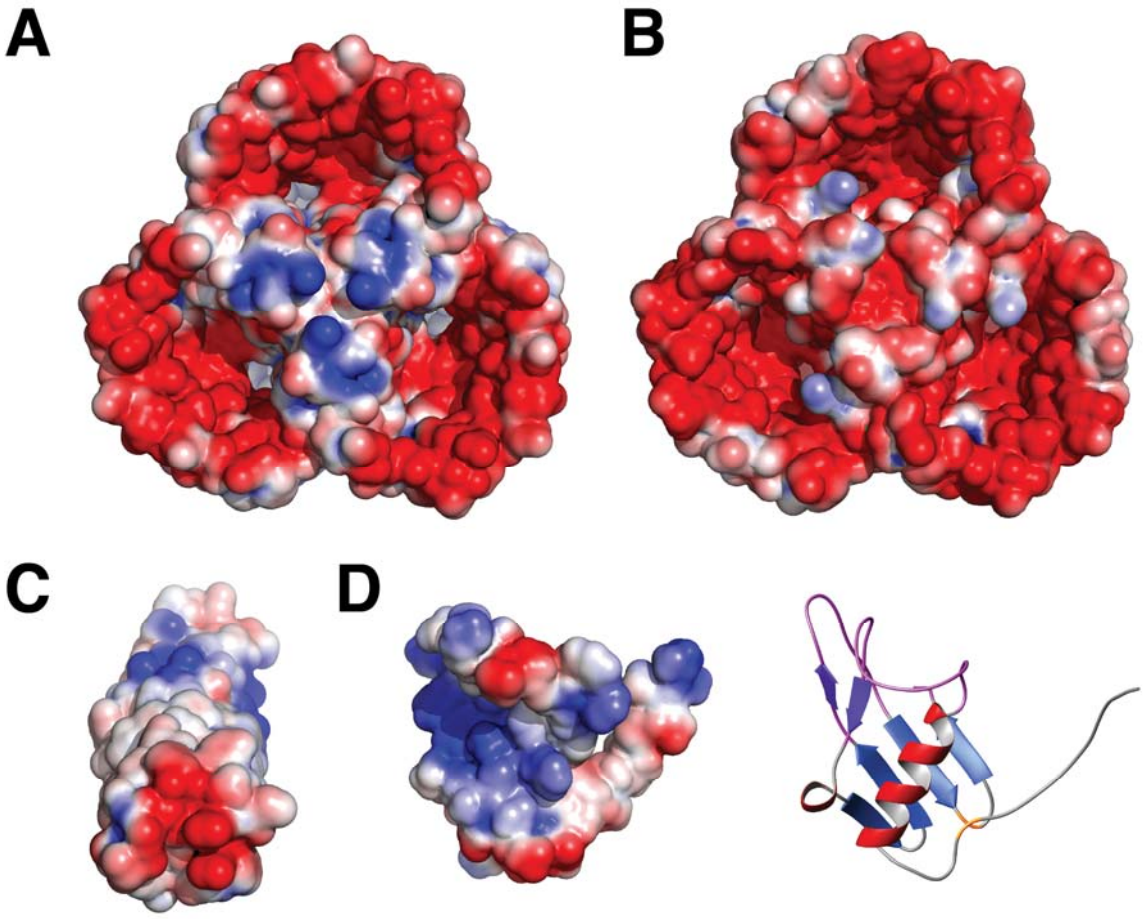

Figure S6, related to Figure 5. Electrostatic Representation of the OmpF and OmpC Periplasmic Face. The surface with electrostatic potential was generated with APBS (Adaptive Poisson-Boltzmann Solver) and pymol. The surface was calculated using the default parameters and the PARSE forcefield. The potential is contoured from -2 kT/e (red) to 2 kT/e (blue). **(A)** The Periplasmic Face of Trimeric OmpF (PDB identifier 1OPF). **(B)** The Periplasmic Face of Trimeric OmpC (PDB identifier 2J1N). **(C)** The Periplasmic face of OmpX (PDB identifier 1QJ8). **(D)** The electrostatic surface representation and ribbon diagram of a low energy YebF structure representative of the ensemble average of residues 22-118. All three Outer membrane protein structures have a negatively charged periplasmic surface complementing the electropositive dynamic regions observed in YebF.

Supplemental Experimental Procedures

Bacterial strains The *E. coli* strains with specific gene deletions used in this study were selected from the Keio Collection (Baba et al., 2006). These were: JW0912 (*ΔompF*), JW2203 (*ΔompC*), JW0799 (*ΔompX*), JW3996 (*ΔlamB*), JW0231 (*ΔphoE*), JW1836 (*ΔyebF*) JW2047 (*Δwza*), JW0146 (*ΔfhuA*) and JW0940 (*ΔompA*). These strains are kanamycin resistant.

Preparation of outer membrane proteins The IM was solubilized by 2% Triton X100. The OM was collected from the above suspension by centrifugation at 40,000 rpm for 60 minutes and solubilized by 3% α-OG (n-octyl-α-D-glucopyranoside, Anatrace) in 20 mM Tris-HCl, pH8.0 for 3 hours. The OM soluble extract was obtained by centrifugation at 40,000 rpm for 60 minutes. Protein concentrations of the OM protein solution were determined by the Bradford method (Bradford, 1976) after removal of detergent by TCA, and finally adjusted to 1.8 mg/mL.

Planar Lipid Bilayer Synthetic 1-palmitoyl-2-oleoyl-sn-glycero-3-phosphoethanolamine (POPE), 1-palmitoyl-2-oleoyl-sn-glycero-3-phosphoserine (POPS), and 1-palmitoyl-2-oleoyl-sn-glycero-3-phosphocholine (POPC) were purchased from Avanti Polar Lipids (Alabaster, USA).

Structure Calculation Backbone dihedral angles were predicted from chemical shifts by TALOS+ (Shen et al., 2009). A disulfide bond between C35 and C108 was introduced based on their $^{13}C\beta$ chemical shifts (diagnostic of the oxidized state) and restraints for the bond generated using CYANA. Hydrogen bond restraints were based on diagnostic NOE patterns. The calculation consisted of 7 cycles of refinement of 100 iterations per cycle (Herrmann et al., 2002). The 10 structures with the lowest calculated target function were chosen as representative of the calculation.

Supplemental References

Baba, T., Ara, T., Hasegawa, M., Takai, Y., Okumura, Y., Baba, M., Datsenko, K.A., Tomita, M., Wanner, B.L., and Mori, H. (2006). Construction of Escherichia coli K-12 in-frame, single-gene knockout mutants: the Keio collection. Mol Syst Biol *2*, 2006 0008.

Bradford, M.M. (1976). A rapid and sensitive method for the quantitation of microgram quantities of protein utilizing the principle of protein-dye binding. Anal Biochem *72*, 248-254.

Farrow, N.A., Muhandiram, R., Singer, A.U., Pascal, S.M., Kay, C.M., Gish, G., Shoelson, S.E., Pawson, T., Forman-Kay, J.D., and Kay, L.E. (1994). Backbone dynamics of a free and phosphopeptide-complexed Src homology 2 domain studied by 15N NMR relaxation. Biochemistry *33*, 5984-6003.

Herrmann, T., Guntert, P., and Wuthrich, K. (2002). Protein NMR structure determination with automated NOE assignment using the new software CANDID and the torsion angle dynamics algorithm DYANA. J Mol Biol *319*, 209-227.

Mulder, F.A., Hon, B., Muhandiram, D.R., Dahlquist, F.W., and Kay, L.E. (2000). Flexibility and ligand exchange in a buried cavity mutant of T4 lysozyme studied by multinuclear NMR. Biochemistry *39*, 12614-12622.

Shen, Y., Delaglio, F., Cornilescu, G., and Bax, A. (2009). TALOS+: a hybrid method for predicting protein backbone torsion angles from NMR chemical shifts. J Biomol NMR *44*, 213-223.

Stoorvogel, J., van Bussel, M.J., and van de Klundert, J.A. (1991). Biological characterization of an Enterobacter cloacae outer membrane protein (OmpX). J Bacteriol *173*, 161-167.

Zhang, G., Brokx, S., and Weiner, J.H. (2006). Extracellular accumulation of recombinant proteins fused to the carrier protein YebF in Escherichia coli. Nat Biotechnol *24*, 100-104.